EXFOLIATED NANOSHEETS OF GRAPHITIC CARBON NITRIDE: STUDY OF OPTICAL AND PHOTOELECTROCHEMICAL PROPERTIES

KOČÍ Kamila[1], RELI Martin[1], SVOBODA Ladislav[1,2], PRAUS Petr[1,2]

VSB - Technical University of Ostrava, [1]Institute of Environmental Technology and [2]Department of Chemistry, Ostrava, Czech Republic, EU,
kamila.koci@vsb.cz

Abstract

The graphitic carbon nitride (g-C_3N_4) samples were prepared by the three different methods: (i) heating of melamine at 600 ºC (bulk g-C_3N_4), (ii) exfoliation of bulk g-C_3N_4 by heating at 500 ºC (Ex500) and (iii) exfoliation of bulk g-C_3N_4 by ultrasonication in an aqueous dispersion (ExUltra). The exfoliation was performed to obtain g-C_3N_4 nanosheets or other nanostructures. The samples characterization was performed by UV-Vis diffuse reflectance (DRS UV-Vis), photoluminescence (PL) spectroscopy and photoelectrochemical (PEC) measurement. The smallest transition energies E_t was evaluated for bulk g-C_3N_4 (E_t = 2.84 eV). The exfoliation by heating and ultrasonication caused both increase of transition energies E_t at 3.07 eV and blue-shift and intensity increase of PL emission bands. The exfoliation by heating at 500 ºC increased photocurrent in comparison with the bulk g-C_3N_4 and ultrasonicated samples. This indicates the beneficial effect of the exfoliation by heating for various photocatalytic applications due to the higher mobility and separation efficiency of photo-induced carriers.

Keywords: Graphitic carbon nitride, optical properties, photoelectrochemical properties

1.   INTRODUCTION

Lately, the graphitic carbon nitride has drawn scientific interest due to its promising role as a visible-light-response photocatalyst (2.7 eV bandgap) for many photocatalytic reactions [1-3]. The energy position of conduction (CB) and valence band (VB) is at –1.1 and 1.6 eV *vs* normal hydrogen electrode (NHE), respectively [3]. Graphitic carbon nitride, a typical metal-free photocatalyst is thermally and chemically stable. Besides, it is very stable under light irradiation in solutions with pH of 0-14 due to the strong covalent bonds between carbon and nitride atoms [4, 5].

Unlike the metal-containing photocatalysts that need expensive metal salts for their preparation, g-C_3N_4 photocatalyst can be facilely prepared by thermally polycondensing of the cheap N-rich precursors, such as dicyanamide, cyanamide, melamine, and urea [3, 6, 7].

These superior properties imply that the metal-free g-C_3N_4 would be an ideal candidate for the design of efficient visible-light-driven photocatalyst such as water splitting, CO_2 photoreduction, organic contaminants purification, catalytic organic synthesis, and fuel cells [1-3, 6-9]. There have been several excellent reviews on g-C_3N_4 preparation and applications in the last 5 years, and readers can refer to these review articles [2, 3, 8, 10] However, pure g-C_3N_4 is far from successful use as an effective photocatalyst due to its lower UV response than pure TiO_2, and its separation efficiency of photoinduced electron-hole pairs still need to be improved [5, 11, 12].

The aim of this work was investigation of optical and photoelectrochemical properties of bulk g-C_3N_4 and g-C_3N_4 nanosheets or other nanostructures prepared by exfoliation of bulk g-C_3N_4 by heating in air and ultrasonication of bulk g-C_3N_4 in the aqueous dispersion.

2. EXPERIMENTAL

2.1. Preparation of graphitic carbon nitride g-C_3N_4

For the study of optical and electrochemical properties three type of graphitic carbon nitride were prepared. The first sample of bulk g-C_3N_4 was prepared through the direct calcination of melamine at 600 ºC for 2 hours. The second sample (Ex500) was prepared by thermal exfoliation of bulk g-C_3N_4 by heating at 500 ºC for 4 hours. The last sample (ExUltra) was prepared by ultrasonic exfoliation of bulk g-C_3N_4 in ultrasonic bath for 1 hour and sequentially filtrated and dried at 100 ºC [13].

2.2. UV-Vis diffuse reflectance

UV-Vis diffuse reflectance spectra were recorded with a Shimadzu UV-2600 (IRS-2600Plus) spectrophotometer at room temperature in the range from 220 nm to 1400 nm. The reflectance was re-calculated to the absorption using the Schuster-Kubelka-Munk equation as follows

$$F(R_{A_i}) = \frac{(1 - R_{A_i})^2}{2R_{A_i}},$$

(1)

where R_{∞} is the diffuse reflectance from a semi-infinite layer. The obtained DRS spectra were transformed to the dependencies of $(F(R_{\infty}) \cdot hv)^2$ on hv in order to obtain transmission energies.

2.3. Photoluminiscence

Photoluminescence spectra were measured by a spectrometer FLS920 (Edinburgh Instrument Ltd, UK). The spectrometer was equipped with a 450 W Xenon lamp (Xe900). The excitation wavelength was 280 nm. The width of excitation and emission slits was 3 nm.

2.4. Photoelectrochemical measurement

Photoelectrochemical experiments (pulsed photocurrent spectroscopy) were performed using a photoelectric spectrometer equipped with the 150 W Xe lamp and coupled with the SP-300 potentiostat. Photocurrent responses were recorded using a classical three electrode setup. The platinum and Ag/AgCl electrodes were used as the auxiliary and reference electrodes, respectively. The working electrode was prepared as follows: TiO_2 powder was deposited onto indium-tin oxide (ITO) coated by polyethylene terephthalate foil. The electrolyte solution was 0.1 M KNO_3. The photocurrent action spectra of the photoelectrode were recorded using pulsed illumination (within the range of 250 - 500 nm with the step of 50 nm) at potentiostatic conditions for different value of applied potentials (from - 0.1 to 0.5 V, step 0.25 V).

3. RESULTS AND DISCUSSION

3.1. UV-Vis diffuse reflectance of prepared materials

For the characterization of prepared materials UV-Vis DRS spectra were recorded in the range from 220 nm to 1400 nm and were evaluated according equation (1). The obtained DRS spectra were transformed to the dependencies of $(F(R_{\infty}) \cdot hv)^2$ on hv in order to obtain transmission energies (**Figure 1**). The magnitudes of transition energy were evaluated at 2.84 eV, 3.07 eV and 3.07 eV for the bulk g-C_3N_4, Ex500 and ExUltra, respectively. The smallest transition energy of bulk g-C_3N_4 (E_t = 2.84 eV) indicates that the exfoliation of bulk g-C_3N_4 caused the shift of absorption edges by 0.23 eV as a result of the formation of g-C_3N_4 nanosheets [14].
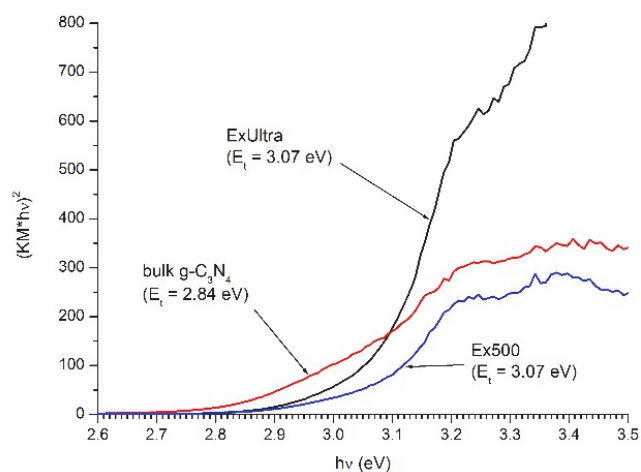
Figure 1 UV-Vis diffuse reflectance spectra of prepared g-C₃N₄ samples

3.2. Photoluminescence analysis of prepared materials

Photoluminescence spectra were recorded in order to characterize the g-C₃N₄ samples as well. **Figure 2** shows emission bands of the bulk g-C₃N₄, Ex500 and ExUltra. The smaller blue-shift of emission bands from 480 nm for bulk g-C₃N₄ to 474 nm for ExUltra and to 463 nm for Ex500 with modification procedure was observed. This result is in agreement with the increasing magnitudes of transition energies. Interrupted parts of the spectra were not measured due to the 2nd order reflection effect of excitation irradiation. The increase of PL intensity of the exfoliated samples was likely caused by cracking of large g-C₃N₄ planes into smaller nanosheets [14].
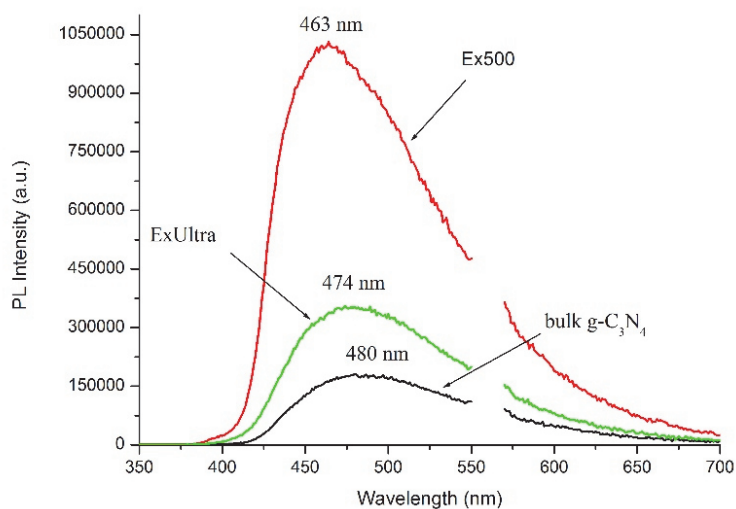

Figure 2 Photoluminescence spectra of prepared g-C₃N₄ samples

3.3. Photoelectrochemical measurement of prepared materials

Photoelectrochemical properties of all prepared g-C₃N₄ samples were examined in order to complete information about their properties. Photocurrent responses were recorded as functions of applied potential and photon energy.

The effectiveness of the photogenerated electron-hole formation in the g-C₃N₄ samples were measured from the photocurrent response under irradiation at the applied potential of 0.5 V vs. Ag/AgCl. **Figure 3** demonstrates the typical real time photocurrent response of the g-C₃N₄ samples when the source of the light

was switched on and off. In semiconductor materials, when irradiation supplies energy is higher than the band gap of a material, the energy excites the electrons from the valence band to the conduction band, leaving a hole in the valence band. This electron-hole pair is responsible for the photocurrent. When the light was turned on, the photocurrent was rapidly increased, and the photocurrent then turned to a steady state after a few seconds. When the light was turned off, the photocurrent decreased [15]. The photocurrent for the Ex500 sample was higher than for the bulk g-C_3N_4 and ExUltra ones when light was on (**Figure 3**). Therefore, the mobility and separation efficiency of the photo-induced carriers were efficaciously improved after heating at 500 ºC of bulk g-C_3N_4.
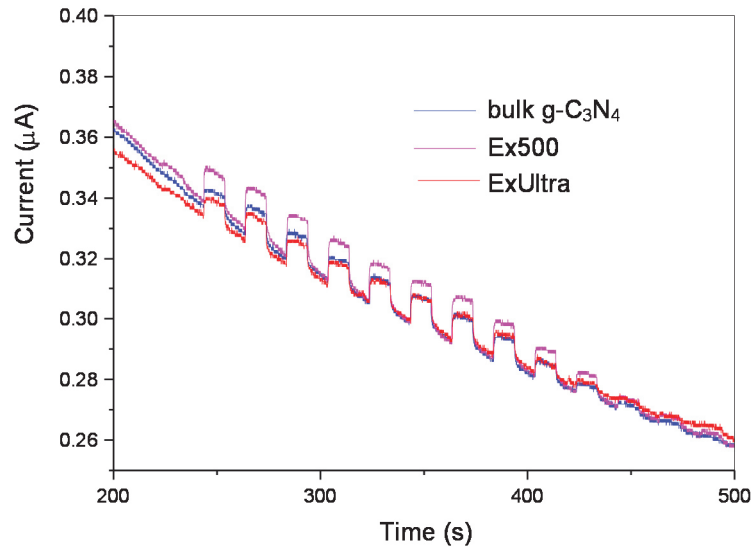

Figure 3 Photocurrent responses spectra of prepared g-C_3N_4 samples

To have a full overview of the photocurrent generation as a function of applied potential and irradiation wavelength a set of photocurrent action spectra was recorded at constant potentials. In this way three-dimensional pictures (phase diagrams or maps) were obtained (**Figure 4**). The photocurrent values were read as a difference between the steady-state current measured upon irradiation and the current in the dark just before opening the shutter. Photocurrent values used for the map construction were not corrected for changes in incident light intensities with irradiation wavelength [16, 17].
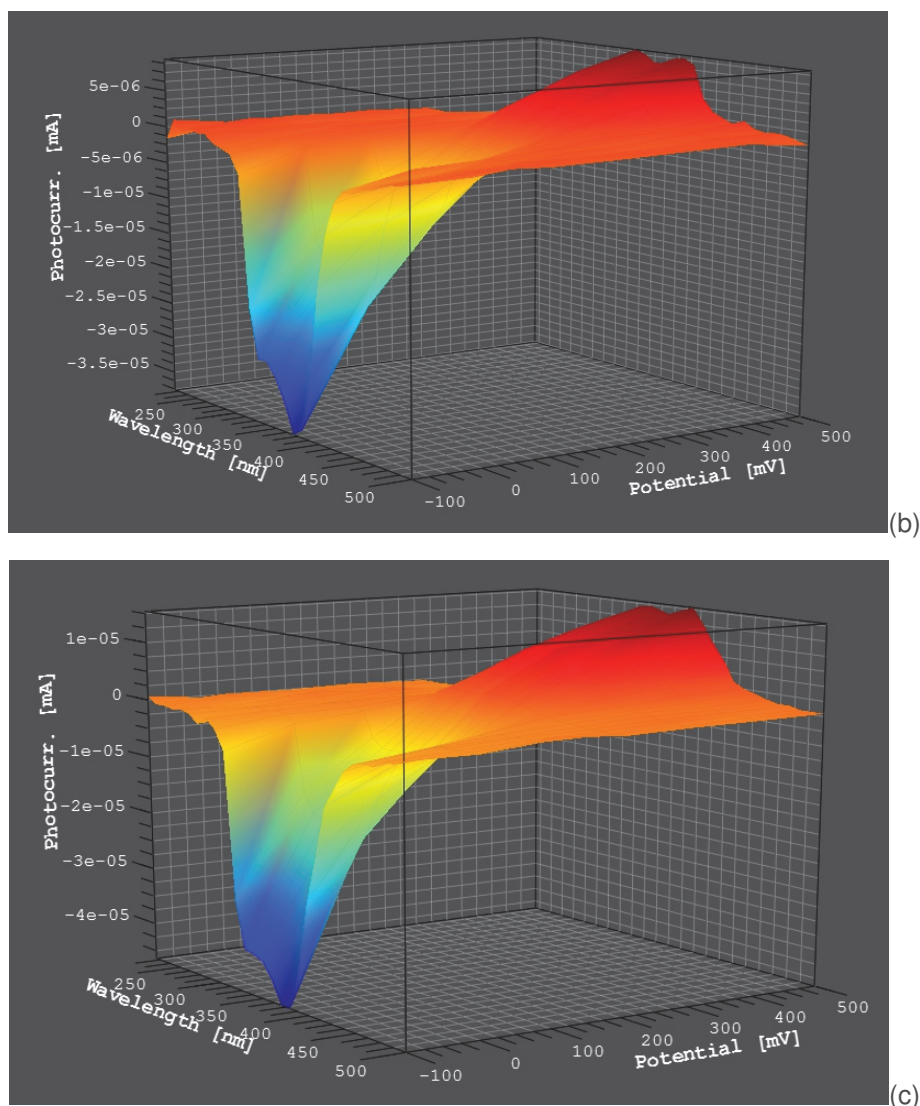

(a)
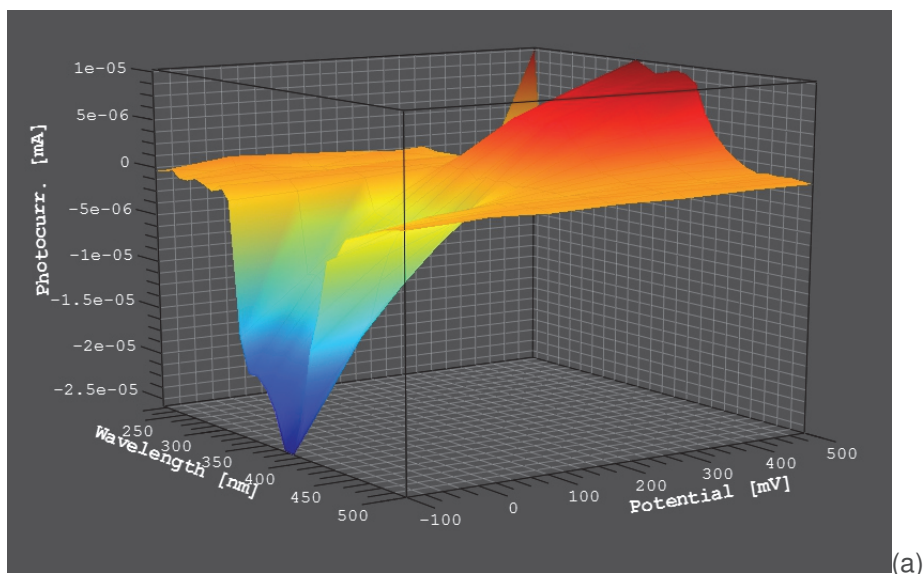
Figure 4 Photocurrents generated at bulk g-C$_3$N$_4$ (a), ExUltra (b) and Ex500 (c) as a function of electrode potential and incident light wavelength

4. CONCLUSION

The g-C$_3$N$_4$ samples were prepared by three different methods (i) heating of melamine at 600 ºC to prepare bulk g-C$_3$N$_4$, and by exfoliation of bulk g-C$_3$N$_4$ into nanosheets by (ii) heating at 500 ºC (Ex500) and (iii) ultrasonication in the aqueous dispersion (ExUltra). Their characterization was performed by the UV-Vis diffuse reflectance, photoluminescence spectroscopy and the photoelectrochemical measurements. The smallest transition energy was evaluated for bulk g-C$_3$N$_4$ (E_t = 2.84 eV). The exfoliation by heating and ultrasonication caused both increasing of transition energies at 3.07 eV and blue-shift and intensity increase of PL emission bands. The g-C$_3$N$_4$ exfoliated at 500 ºC provided the highest photocurrent in comparison with bulk g-C$_3$N$_4$ and ExUltra. This indicates the beneficial effect of the exfoliation by heating for possible photocatalytic applications due to the high mobility and separation efficiency of the photo-induced carriers. The detail analysis of optical and electron properties as well as the relationship between them is very attractive and will be studied in the future. It is supposed to bring new important knowledge that will be used in optimizing the performance of photochemical systems and in the description of key properties related to many photocatalytic reactions.

ACKNOWLEDGEMENTS

REFERENCES

[1]   Y. GONG, M. LI, Y. WANG, Carbon nitride in energy conversion and storage: recent advances and future prospects, ChemSusChem, 8 (2015) 931-946.

[2]   S. CAO, J. LOW, J. YU, M. JARONIEC, Polymeric photocatalysts based on graphitic carbon nitride, Adv. Mater., 27 (2015) 2150-2176.

[3]   S. YE, R. WANG, M.-Z. WU, Y.-P. YUAN, A review on g-C3N4 for photocatalytic water splitting and CO2 reduction, Applied Surface Science, 358 (2015) 15-27.

[4]   G. LIAO, S. CHEN, X. QUAN, H. YU, H. ZHAO, Graphene oxide modified g-C3N4hybrid with enhanced photocatalytic capability under visible light irradiation, J. Mater. Chem., 22 (2012) 2721-2726.

[5]   J. LI, Y. LIU, H. LI, C. CHEN, Fabrication of g-C3N4/TiO2 composite photocatalyst with extended absorption wavelength range and enhanced photocatalytic performance, Journal of Photochemistry and Photobiology A: Chemistry, 317 (2016) 151-160.

[6]   S.C. YAN, Z.S. LI, Z.G. ZOU, Photodegradation performance of g-C3N4 fabricated by directly heating melamine, Langmuir, 25 (2009) 10397-10401.

[7]   F. DONG, L. WU, Y. SUN, M. FU, Z. WU, S.C. LEE, Efficient synthesis of polymeric g-C3N4 layered materials as novel efficient visible light driven photocatalysts, J. Mater. Chem., 21 (2011) 15171.

[8]   F. CHANG, Y. XIE, C. LI, J. CHEN, J. LUO, X. HU, J. SHEN, A facile modification of g-C3N4 with enhanced photocatalytic activity for degradation of methylene blue, Applied Surface Science, 280 (2013) 967-974.

[9]   F. JIANG, T. YAN, H. CHEN, A. SUN, C. XU, X. WANG, A g-C3N4-CdS composite catalyst with high visible-light-driven catalytic activity and photostability for methylene blue degradation, Applied Surface Science, 295 (2014) 164-172.

[10]   S. CAO, J. YU, g-C3N4-Based Photocatalysts for Hydrogen Generation, J Phys Chem Lett, 5 (2014) 2101-2107.

[11]   S. ZHAO, S. CHEN, H. YU, X. QUAN, g-C3N4/TiO2 hybrid photocatalyst with wide absorption wavelength range and effective photogenerated charge separation, Sep. Purif. Technol., 99 (2012) 50-54.

[12]   J. LI, B. SHEN, Z. HONG, B. LIN, B. GAO, Y. CHEN, A facile approach to synthesize novel oxygen-doped g-C3N4 with superior visible-light photoreactivity, Chem Commun (Camb), 48 (2012) 12017-12019.

[13]   P. PRAUS , L. SVOBODA, B. SMETANA, Exfoliated nanosheets of graphitic carbon nitride: Study of structure and morphology, NANOCON 2016: 8th International Conference of Nanomaterials-Research & Application, (2016) submitted.

[14]   P. NIU, L. ZHANG, G. LIU, H.-M. CHENG, Graphene-Like Carbon Nitride Nanosheets for Improved Photocatalytic Activities, Adv. Funct. Mater., 22 (2012) 4763-4770.

[15]   J.H. LEE, H. LEE, M. KANG, Remarkable photoconversion of carbon dioxide into methane using Bi-doped TiO2 nanoparticles prepared by a conventional sol-gel method, Materials Letters, 178 (2016) 316-319.

[16]   G.Y.S. MACIEJ HEBDA, KONRAD SZACIŁOWSKI, WOJCIECH MACYK, Optoelectronic Switches Based on Wide Band Gap Semiconductors, J. Phys. Chem. B, 110 (2006) 15275-15283.

[17]   K. SZACIŁOWSKI, W. MACYK, Chemical switches and logic gates based on surface modified semiconductors, Comptes Rendus Chimie, 9 (2006) 315-324.